On the signal contribution function with respect to different norms

Klaus Neymeyr[a,b], Mathias Sawall[a], Alejandro C. Olivieri[c]

[a] *Universität Rostock, Institut für Mathematik, Ulmenstrasse 69, 18057 Rostock, Germany*
[b] *Leibniz-Institut für Katalyse, Albert-Einstein-Strasse 29a, 18059 Rostock*
[c] *Universidad Nacional de Rosario, Departamento de Química Analítica, Suipacha 531, Rosario S2002LRK, Argentina*

Abstract

The signal contribution function (SCF) in multivariate curve resolution evaluates signal portions of specific components either in absolute or in relative form related to the integrated signal of all components. In 1999 Gemperline used the summed signal data and in 2001 Tauler worked with the square-summed relative signal in order to determine the profiles that minimize respectively maximize the signal contribution. These profiles approximate the bands of all feasible profiles. Here Gemperline's approach using the entrywise 1-matrix norm is proved to provide accurate bounds for two-component systems. This revives the approach of summed mass or absorption values with its potentially better chemical interpretability.

Key words: signal contribution function, multivariate curve resolution, Borgen plot, Area of feasible solutions, MCR-Bands

1. Introduction

Pure component decompositions in chemometrics aim at determining matrix factorizations $D = CS^T$, namely to factorize a given spectral data matrix D into the pure component factors C and S. The chemically true factorization provides in the columns of C the concentration profiles of the pure components along the time axis. The corresponding columns of S are the associated pure component spectra. However, the factorization problem suffers from ambiguous factors. The non-unique profiles can be represented by the so-called bands of feasible solutions. Gemperline in 1999 [5] and later Tauler in 2001 [25] suggested techniques to measure the extent of the factor ambiguity by determining the minimal and maximal contribution of a constituent to the total signal. The related profiles of minimal and maximal signal contribution approximate to a certain extent the boundaries of the bands of feasible solutions. They can even reproduce the band boundaries exactly in certain cases. If c_ℓ is the concentration profile of a certain chemical species and if s_ℓ is the associated spectrum, then the rank-1 matrix $c_\ell s_\ell^T$ represents the contribution of the species ℓ to the k-by-n matrix D of mixture data. If C and S contain columnwise the pure component information, then $c_\ell = C(:,\ell)$ and $s_\ell = S(:,\ell)$ represent the contribution by the ℓth chemical species.

Gemperline by Equation (8) of [5] suggested to determine the minimum and maximum of the summed up or integrated signal

$$\text{minimum or maximum of } \sum_{i=1}^{k}\sum_{j=1}^{n}(c_\ell)_i(s_\ell)_j \tag{1}$$

subject to the feasible nonnegative concentration profiles and the associated spectral profiles. Tauler by Equation (6) of [25] suggested to analyze the signal contribution in a relative fashion related to the total absorption $D = CS^T$, namely to determine the minimum and maximum of the signal contribution function (SCF)

$$\frac{\|c_\ell s_\ell^T\|_F}{\|CS^T\|_F}. \tag{2}$$

Therein $\|\cdot\|_F$ denotes the Frobenius norm, that is the square root of the sum-of-squares (ssq) of all matrix elements. Tauler gave as an argument for the use of the Frobenius norm, that "*for some spectroscopic signals giving negative values, Equation* (2) *should be preferred since it is valid also for negative profiles*". However, using sums of squares is not the only way to work with partially negative data. An alternative is to use absolute values in Gemperline's approach (1), namely to consider sums of $|c_\ell|_i|s_\ell|_j$. This amounts to substituting the Frobenius norm of cs^T in (2) by the entrywise 1-norm. This substitution rises the general question which norms can be useful in the definition of general signal contribution functions.

The choice of norm in (2) has not yet been systematically analyzed. In most cases the Frobenius norm has been used, see, e.g., the analyses in [1, 2, 17, 12] and the MCR-Bands software [9]. However, mathematics provides

(infinitely) many other vector and matrix norms. An influence of different normalizations on the results of multivariate curve resolution calculations is a known phenomenon. It has been studied, e.g., in the context of factor ambiguities by Borgen and Kowalski [4] and systematically under the keyword Borgen norms by Rajkó [16]. Further, sparsity is sometimes used as a constraint in multivariate curve resolution methods and works with the 1-norm or even the 0-norm, which counts the number of non-zero entries of a vector [14]. Here, we focus on the 1-norm and the maximum norm which reads for vectors x

$$\|x\|_1 = \sum_i |x_i|, \qquad \|x\|_\infty = \max_i |x_i|.$$

Different norms relate to different ways of measuring distances. Changing the matrix norm in the definition of the SCF can help to extract different chemical meanings and can potentially open up new chemical interpretations. For instance, the 1-norm of a spectral profile measures the summed up absorption along the frequency axis. Correspondingly, the 1-norm of a concentration profile vector relates to the time integral of the concentration profile. Alternatively, the maximum norm yields maximal absorption or concentration values.

1.1. Overview

Section 2 introduces various vector and matrix norms and determines the componentwise 1-norm as a proper candidate for the mathematical analysis of the maximum and minimum of the SCF. This approach complies for nonnegative profiles with the signal sums used by Gemperline. Section 3 proves that the SCF for the entrywise 1-norm and for systems with two species takes its maximum and minimum in profiles that include the ranges of all feasible profiles. Section 4 points out that a comparable analysis for the entrywise maximum norm leads to mathematical difficulties that cannot be easily overcome. Numerical studies are presented in Section 5.

2. The SCF for different matrix norms

We start with considering the square sum signal integration as suggested by Tauler according to (2). The numerator of (2) satisfies (we omit the index ℓ of the chemical species)

$$\|cs^T\|_F^2 = \sum_{i=1}^{k}\sum_{j=1}^{n}\left((cs^T)_{ij}\right)^2 = \sum_{i=1}^{k} c_i^2 \sum_{j=1}^{n} s_j^2 = \|c\|_2^2\,\|s\|_2^2.$$

In words, the Frobenius norm of $cs^T \in \mathbb{R}^{k\times n}$ factorizes into the product of the Euclidean vector norms of c and s. From a mathematical point of view these squared Euclidean norms have the advantage that they allow us to compute partial derivatives of the SCF with respect to the vector components c_i and s_i. The partial derivatives are the basis of the analysis in [12] for finding minima and maxima of the SCF. For chemical systems with two chemical species the two extrema of the SCF are proved to be associated with profiles that enclose the ranges of all feasible profiles [12]. Next we investigate the SCF with respect to other norms.

2.1. The SCF for the 1-matrix norm

An alternative to the Frobenius norm is the 1-*matrix* norm. For a general k-by-n matrix M this norm is defined by means of the 1-*vector* norm $\|x\|_1 = \sum_i |x_i|$ as follows

$$\|M\|_1 = \max_{x\neq 0} \frac{\|Mx\|_1}{\|x\|_1} = \max_{1\le j\le n} \sum_{i=1}^{k} |m_{ij}|. \tag{3}$$

See Sec. 2.3.2 in [8] for details. In words, the 1-operator norm of M is the maximal absolute sum along the columns. Hence this norm is also called the *column-sum-norm*. The direct computation

$$\|cs^T\|_1 = \max_{1\le j\le n} \sum_{i=1}^{k} |c_i s_j| = \sum_{i=1}^{k} |c_i| \cdot \max_{1\le j\le n} |s_j| = \|c\|_1\,\|s\|_\infty \tag{4}$$

shows that the 1-operator norm of cs^T equals the product of the 1-vector norm of c and the maximum norm of s. Thus c and s are evaluated with respect to different vector norms. As c and s are assumed to be nonnegative vectors, we get that

$$\|c\|_1 = c_1 + \cdots + c_k, \qquad \|s\|_\infty = \max_{1\le j\le n} s_j. \tag{5}$$

Having in mind our goal to determine maxima and minima of $\|cs^T\|_1$ with respect to the choice of c and s, we note that $c_1 + \cdots + c_k$ is a differentiable function with respect to all its components c_i and that nonnegativity has allowed us to get rid of the non-differentiable absolute value function. Unfortunately, the maximum underlying the definition of $\|s\|_\infty$ is not a differentiable function of s_i which prevents forming the partial derivatives.

2.2. The SCF for the maximum matrix norm

The maximum *vector* norm $\|x\|_\infty = \max_i |x_i|$ is the basis to defining the *matrix* norm

$$\|M\|_\infty = \max_{x\neq 0} \frac{\|Mx\|_\infty}{\|x\|_\infty} = \max_{1\leq i\leq k} \sum_{j=1}^{n} |m_{ij}|. \tag{6}$$

Again, see [8] for the last equality. Thus $\|M\|_\infty$ is the maximal absolute row sum of M and is called the row-sum norm. The evaluation of cs^T with respect to the row-sum norm and $c, s \geq 0$ yield

$$\|cs^T\|_\infty = \max_{1\leq i\leq n} \sum_{j=1}^{k} |c_i s_j| = \max_{1\leq i\leq k} c_i \cdot \sum_{j=1}^{n} s_j = \|c\|_\infty \|s\|_1. \tag{7}$$

In analogy to (5), the maximum norm of c prevents taking partial derivatives for finding extrema of the SCF. For this reason we do not pursue an analysis of the SCF with respect to the column-sum or row-sum norms.

2.3. The SCF for the entrywise 1-norm

The entrywise 1-norm (which we write by a triple-lined norm symbol)

$$|||M|||_1 = \sum_{i=1}^{k} \sum_{j=1}^{n} |m_{ij}| \tag{8}$$

is also a matrix norm. One can easily check the three norm axioms: First, the positive definiteness ($|||M|||_1 \geq 0$, $|||M|||_1 = 0$ if and only if $M = 0$). Second, the absolute homogeneity ($|||\lambda M|||_1 = |\lambda| \cdot |||M|||_1$ for all real numbers λ). Third, the triangle inequality ($|||M + N|||_1 \leq |||M|||_1 + |||N|||_1$ for all k-by-n matrices M and N). In contrast to the column sum norm, the entrywise 1-norm is not an operator norm. This means that no vector norm $\|\cdot\|$ exists so that $|||M|||_1 = \max_{x\neq 0} \|Mx\|/\|x\|$ for general M. The latter statement is true since for the $n \times n$ identity matrix $M = I$ we get $|||I|||_1 = n$, but for any vector norm it holds that $\|Ix\|/\|x\| = 1$ so that any operator norm of I equals 1.

The entrywise 1-norm of cs^T reads for nonnegative c and s

$$|||cs^T|||_1 = \sum_{i=1}^{k} \sum_{j=1}^{n} |c_i s_j| = \|c\|_1 \|s\|_1 = \sum_{i=1}^{k} c_i \sum_{j=1}^{n} s_j. \tag{9}$$

The entrywise 1-norm of cs^T evaluates the 1-norms of c and s. The last equality is valid for nonnegative c and s and amounts to the summed signal approach by Gemperline, see Eq. (1). In contrast to the norms discussed in Sections 2.1 and 2.2 the norm is symmetric in the sense that $|||cs^T|||_1 = |||sc^T|||_1$. Additionally, the entrywise 1-norm of cs^T is a differentiable function of c and s on the assumption of their nonnegativity. This qualifies the entrywise 1-norm as a promising alternative for the mathematical analysis. The two 1-vector norms measure chemically interpretable quantities which is discussed in the next section.

2.4. Chemical interpretation of the various norms

Next we interpret the chemical meaning of the three matrix norms, namely the matrix 1-norm, the matrix maximum norm and the entrywise matrix 1-norm: From the perspective of analytical chemists the 1-norm of a concentration vector, which represents a concentration profile along the time coordinate, is a time-sum of concentration values. Hence uncertainties due to the rotational ambiguity appearing in the bands of feasible solutions are proportional to uncertainties of the concentration values. A similar interpretation of the 1-norm is possible for the spectral profiles and the associated absorption values. The two matrix norms (3) and (6), see Sections 2.1 and 2.2, seem to be less suitable for a chemical interpretation since a 1-norm for one vector and the maximum norm for the other vector are to be evaluated, see Eqns. (4) and (7). This breaks a symmetric treatment of the two factors. On the one hand, the maximum norm of a concentration profile or a spectrum, that is the maximal absolute value of its components, is potentially sensitive to perturbed data or experimental data with outliers. On the other hand, the 1-norm sums up or averages the components and thus seems to be less sensitive to noise. This leads us to the analysis of the entrywise 1-norm in the following section.

A further possible approach is to determine the profiles that maximize or minimize the relative signal contribution according to

$$\|c\|/\|C\| \quad \text{subject to} \quad \|s_\ell\|_2 = 1 \text{ for all } \ell \text{ species}. \tag{10}$$

Therein $\|\cdot\|$ can be any norm, e.g. the 1-vector norm in the numerator and the associated 1-matrix norm in the denominator. Then $\|c\|/\|C\|$ is a relative contribution measure with numerical values between 0 and 1. The key concept behind (10) is a normalization of the associated spectrum with respect to the Euclidean norm. However, such an approach is not consistent with the evaluation of $\|cs^T\|$ for general norms. Hence we do not pursue Eq. (10) or its variant with swapped positions of the concentration factor and spectral factor any further.

3. The SCF for the entrywise 1-norm and two-component systems

The subsequent analysis of the SCF with respect to the entrywise 1-norm follows the general procedure as used in [12, 17] and which is based on the Frobenius norm. All arguments are to be adapted to the present norm. The starting point is the fact that any nonnegative factorization $D = CS^T$ can be represented by a truncated singular value decomposition (SVD) $D = U\Sigma V^T$ with $U \in \mathbb{R}^{k\times s}$, $\Sigma \in \mathbb{R}^{s\times s}$ and $V \in \mathbb{R}^{n\times s}$ and a regular matrix $T \in \mathbb{R}^{s\times s}$ so that $C = U\Sigma T^{-1}$ and $S^T = TV^T$. The first column of T can be used to fix a certain normalization of the profiles. The matrix can be written in the 2×2 block form

$$T = \begin{pmatrix} 1 & x \\ \mathbf{1} & W \end{pmatrix} \tag{11}$$

with $x = (x_1, \ldots, x_{s-1})$, $W \in \mathbb{R}^{s-1\times s-1}$ and the all-ones vector $\mathbf{1} = (1, \ldots, 1)^T \in \mathbb{R}^{s-1}$, see [4, 22]. The vector x has a key position. Any x which can be extended to a regular matrix T according to (11) so that C and S are nonnegative matrices is called a feasible profile. The set of all those x represents the ambiguity underlying the factorization problem and is called the Area of Feasible Solution (AFS)

$$\mathcal{M}_S = \left\{ x \in \mathbb{R}^{s-1} : \ W \in \mathbb{R}^{(s-1)\times(s-1)} \text{ exists in (11) so that } T \text{ is regular and } C, S \geq 0 \right\}.$$

Geometric construction techniques for the AFS are described in [4, 18, 10, 19], whereas [6, 7, 20, 22, 23] report on numerical approximation techniques.

3.1. Mathematical analysis

In order to determine the extrema of $|||c_\ell s_\ell^T|||_1 / |||CS^T|||_1$ we use the T-dependent representations $c_\ell = U\Sigma T^{-1}(:, \ell)$ and $s_\ell^T = (T(\ell, :))V^T$. The denominator does not depend on T which allows us to restrict the optimization of the function

$$g_\ell(T) = \left|\left| U\Sigma(T^{-1}(:, \ell))(T(\ell, :))V^T \right|\right|_1 . \tag{12}$$

For two-component systems the 2×2 matrix T and its inverse read

$$T = \begin{pmatrix} 1 & \alpha \\ 1 & \beta \end{pmatrix}, \qquad T^{-1} = \frac{1}{\beta - \alpha} \begin{pmatrix} \beta & -\alpha \\ -1 & 1 \end{pmatrix}, \tag{13}$$

where $\alpha \neq \beta$ is assumed in order to guarantee the invertibility of T; otherwise the factors would not have the rank 2. Hence we get $C \in \mathbb{R}^{k\times 2}$ and $S \in \mathbb{R}^{n\times 2}$ (with $U = [u_1, u_2]$ and $V = [v_1, v_2]$) as

$$\begin{aligned} C = (c_1, c_2) = U\Sigma T^{-1} &= \frac{1}{\beta - \alpha} \left(\beta\sigma_1 u_1 - \sigma_2 u_2, -\alpha\sigma_1 u_1 + \sigma_2 u_2\right), \\ S^T = \begin{pmatrix} s_1^T \\ s_2^T \end{pmatrix} = TV^T &= \begin{pmatrix} 1 & \alpha \\ 1 & \beta \end{pmatrix} \begin{pmatrix} v_1^T \\ v_2^T \end{pmatrix} = \begin{pmatrix} v_1^T + \alpha v_2^T \\ v_1^T + \beta v_2^T \end{pmatrix}. \end{aligned} \tag{14}$$

Equation (12) for $\ell = 1$ yields with $g_1(T) = g_1(\alpha, \beta)$

$$g_1(\alpha, \beta) = \|c_1\|_1 \|s_1\|_1 = \frac{1}{\beta - \alpha} \|\beta\sigma_1 u_1 - \sigma_2 u_2\|_1 \|v_1 + \alpha v_2\|_1 . \tag{15}$$

Since c_1 and s_1 are componentwise nonnegative vectors for feasible T, the absolute values can be omitted in the evaluation of the 1-norms. This leads to

$$\begin{aligned} g_1(\alpha, \beta) &= \frac{1}{\beta - \alpha} \Big(\sum_{i=1}^{k} \underbrace{\beta\sigma_1 \overbrace{U_{i1}}^{>0} - \sigma_2 U_{i2}}_{\geq 0} \Big) \Big(\sum_{j=1}^{n} \underbrace{\overbrace{V_{j1}}^{>0} + \alpha V_{j2}}_{\geq 0} \Big) \\ &= \frac{1}{\beta - \alpha} \Big(\beta\sigma_1 \|u_1\|_1 - \sigma_2 \sum_{i=1}^{k} U_{i2} \Big) \Big(\|v_1\|_1 + \alpha \sum_{j=1}^{n} V_{j2} \Big) \end{aligned}$$

where we have used the fact that the singular vectors $U(:, 1) = u_1$ and $V(:, 1) = v_1$ corresponding to the largest singular value σ_1 can be assumed to be componentwise positive. (For details on this fact see [26] where the Perron-Frobenius spectral theory applied to $D^T D$ and DD^T shows that the components of the eigenvectors belonging to the largest eigenvalues all have the same sign. Without loss of generality this sign can be assumed to be positive. The case of in all components negative vectors can be treated by substituting $u_1 \to -u_1$ and $v_1 \to -v_1$.)

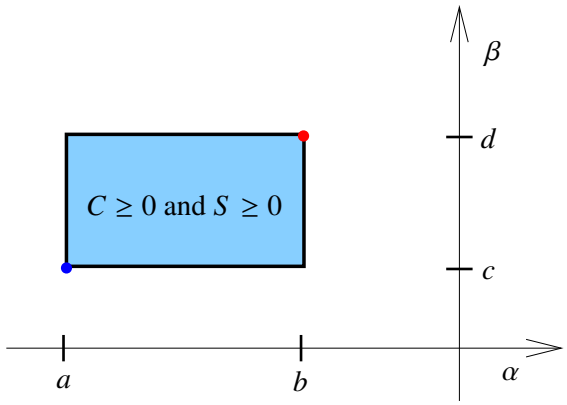

Figure 1: Rectangular feasible region $[a,b]\times[c,d]$ in which $C\geq 0$ and $S\geq 0$ holds according to (17). The SCF minimum at (a,c) is marked by a blue dot and the maximum at (b,d) by a red dot.

In the second case $\ell=2$ we get similar results. For the nonnegative profiles c_2 and s_2 it holds that

$$\begin{aligned} g_2(\alpha,\beta) &= \|c_2\|_1\|s_2\|_1 = \frac{1}{\beta-\alpha}\|\underbrace{-\alpha\sigma_1 u_1+\sigma_2 u_2}_{\geq 0}\|_1\|\underbrace{v_1+\beta v_2}_{\geq 0}\|_1 \\ &= \frac{1}{\beta-\alpha}\Big(-\alpha\sigma_1\|u_1\|_1+\sigma_2\sum_{i=1}^{k}U_{i2}\Big)\Big(\|v_1\|_1+\beta\sum_{j=1}^{n}V_{j2}\Big) \\ &= \frac{1}{\alpha-\beta}\Big(\alpha\sigma_1\|u_1\|_1-\sigma_2\sum_{i=1}^{k}U_{i2}\Big)\Big(\|v_1\|_1+\beta\sum_{j=1}^{n}V_{j2}\Big) \\ &= g_1(\beta,\alpha). \end{aligned}$$

Thus an extremum of $g_1(\alpha,\beta)$ is an extremum of $g_2(\beta,\alpha)$ and vice versa. This justifies to restrict the following analysis on g_1.

3.2. The SCF takes its extrema at the vertices of the rectangle of feasible solutions

The nonnegativity of $C=U\Sigma T^{-1}$ and $S=VT^T$ with T and its inverse given by (13) imposes the following restrictions on (α,β)

$$(\alpha,\beta)\in[a,b]\times[c,d] \quad \text{or} \quad (\beta,\alpha)\in[a,b]\times[c,d], \tag{16}$$

with

$$a=-\min_{\substack{V_{i2}>0\\ i=1,\ldots,n}}\frac{V_{i1}}{V_{i2}}, \quad b=\min_{i=1,\ldots,k}\frac{U_{i2}\sigma_2}{U_{i1}\sigma_1}<0, \quad c=\max_{i=1,\ldots,k}\frac{U_{i2}\sigma_2}{U_{i1}\sigma_1}>0, \quad d=-\max_{\substack{V_{i2}<0\\ i=1,\ldots,n}}\frac{V_{i1}}{V_{i2}}, \tag{17}$$

see, e.g., Sec. 3.6 in [22] for the determination of the constants a, b, c and d. Figure 1 illustrates the rectangular region with $C\geq 0$ and $S\geq 0$. Again, the second alternative in (16) reflects the symmetry of g_1 and g_2 with respect to its arguments. Next we determine the extrema of g_1. A vanishing gradient of g_1

$$\begin{aligned} \nabla g_1 &= \left(\frac{\partial g_1}{\partial\alpha},\ \frac{\partial g_1}{\partial\beta}\right)^T \\ &= \frac{1}{(\beta-\alpha)^2}\begin{pmatrix}\Big(\beta\sigma_1\|u_1\|_1-\sigma_2\sum_{i=1}^{k}U_{i2}\Big)\Big(\|v_1\|_1+\beta\sum_{j=1}^{n}V_{j2}\Big)\\ -\Big(\alpha\sigma_1\|u_1\|_1-\sigma_2\sum_{i=1}^{k}U_{i2}\Big)\Big(\|v_1\|_1+\alpha\sum_{j=1}^{n}V_{j2}\Big)\end{pmatrix}=0 \end{aligned} \tag{18}$$

is a necessary condition for a local extremum of g_1 in (α,β). The condition (18) is symmetric in α and β. First, we treat the singular case $\sum_j V_{j2}=0$. Then $\nabla g_1=0$ can only be fulfilled for $\alpha=\beta$ which is impossible for C and S having the rank 2. Thus this case is not consistent with a local extremum in $[a,b]\times[c,d]$. Second, the general case $\sum_j V_{j2}\neq 0$ leaves for $\alpha\neq\beta$ the two possibilities

$$(\alpha,\beta) \quad \text{or} \quad (\beta,\alpha) \quad \text{equals} \quad \left(\frac{\sigma_2\sum_{i=1}^{k}U_{i2}}{\sigma_1\|u_1\|_1},\ \frac{-\|v_1\|_1}{\sum_{j=1}^{n}V_{j2}}\right).$$

Our aim is to show that α and β in a point of a maximum or minimum of the SCF can only attain the endpoints a, b, c and d (and not values in the interior of the intervals $[a, b]$ and $[c, d]$. We start with the case that α or β equal the value $(\sigma_2/\sigma_1)\sum_{i=1}^{k} U_{i2}/\|u_1\|_1$. Inequality (24) from Appendix A proves that the following inequality is true

$$b = \left(\frac{\sigma_2}{\sigma_1}\right) \min_{i=1,\dots,k} \frac{U_{i2}}{U_{i1}} \leq \underbrace{\left(\frac{\sigma_2}{\sigma_1}\right) \frac{\sum_{i=1}^{k} U_{i2}}{\|u_1\|_1}}_{\alpha \text{ or } \beta} = \left(\frac{\sigma_2}{\sigma_1}\right) \frac{U_{12} + \dots U_{k2}}{U_{11} + \dots U_{k1}} \leq \left(\frac{\sigma_2}{\sigma_1}\right) \max_{i=1,\dots,k} \frac{U_{i2}}{U_{i1}} = c. \tag{19}$$

Together with the conditions (16) and (17) we conclude that only the endpoints b and c satisfy the inequalities above and simultaneously guarantee that C and S are nonnegative.

Next, we consider the alternative case that α or β attain the coordinate $-\|v_1\|_1/\sum_{j=1}^{n} V_{j2}$ in order to attain a vanishing gradient in (18). We have to distinguish the two cases $\sum_{j=1}^{n} V_{j2}$ being larger or less than zero (and refer to the discussion above showing that the sum can never equal zero). If $\sum_{j=1}^{n} V_{j2} > 0$, then a proof is given that shows

$$\frac{-\|V(:,1)\|_1}{\sum_{j=1}^{n} V_{j2}} \leq -\min_{\substack{V_{i2}>0 \\ i=1,\dots,n}} \frac{V_{i1}}{V_{i2}} = a$$

or equivalently

$$\min_{\substack{V_{i2}>0 \\ i=1,\dots,n}} \frac{V_{i1}}{V_{i2}} \leq \frac{\|V(:,1)\|_1}{\sum_{j=1}^{n} V_{j2}}. \tag{20}$$

In the other case $\sum_{j=1}^{n} V_{j2} < 0$ we have to show

$$\frac{-\|V(:,1)\|_1}{\sum_{j=1}^{n} V_{j2}} \geq -\max_{\substack{V_{i2}<0 \\ i=1,\dots,n}} \frac{V_{i1}}{V_{i2}} = d \tag{21}$$

or equivalently

$$\frac{\|V(:,1)\|_1}{\sum_{j=1}^{n} V_{j2}} \leq \max_{\substack{V_{i2}<0 \\ i=1,\dots,n}} \frac{V_{i1}}{V_{i2}}. \tag{22}$$

The two inequalities (20) and (22) are proved in Theorem A.2 by inequalities (27) and (28). Together with the nonnegativity constraints, which force α and β to stay in the intervals $[a, b]$ respectively $[c, d]$, this proves that a maximum or minimum of the SCF can only be attained in the endpoint coordinates a, b, c or d.

The following properties of the SCF (15) follow from the analysis above:

1. The SCF (15) takes its minimum in the vertex (a, c) and its maximum in the vertex (b, d).

   Proof. The assertion follows by proving that

   $$\frac{\partial}{\partial\alpha} g_1 > 0 \quad \text{and} \quad \frac{\partial}{\partial\beta} g_1 > 0 \quad \text{for} \quad (\alpha,\beta) \in (a, b) \times (c, d).$$

   First, according to (18) it holds that $\partial g_1/\partial\beta = \omega(\sigma_2 \sum_{i=1}^{k} U_{i2} - \alpha\sigma_1\|u_1\|_1)$ for a positive constant ω; the constant includes the factor $\|v_1\|_1 + \alpha\sum_{j=1}^{n} V_{j2}$ which equals the positive componentwise sum of s_2. Thus it remains to show

   $$\frac{\sigma_2 \sum_{i=1}^{k} U_{i2}}{\sigma_1 \sum_{i=1}^{k} U_{i1}} > \alpha \in (a, b),$$

   which has already been proved by (19).
   Second, according to (18) it holds that $\partial g_1/\partial\alpha = \bar{\omega}(\|v_1\|_1 + \beta\sum_{j=1}^{n} V_{j2})$ for a positive constant $\bar{\omega}$ which includes as a factor the positive componentwise sum of s_1. It remains to show that $\|v_1\|_1 + \beta\sum_{j=1}^{n} V_{j2} > 0$. By following the argumentation around Eqns. (20)–(22) we distinguish the three cases $\sum_{j=1}^{n} V_{j2} > 0$, equal to 0 or less than 0. The case of equality to 0 has already been shown to contradict the necessary condition $\alpha \neq \beta$. If $\sum_{j=1}^{n} V_{j2} > 0$, then it remains to show that $\beta > -\|v_1\|_1/\sum_{j=1}^{n} V_{j2}$ which has already been proved since

   $$-\frac{\|v_1\|_1}{\sum_{j=1}^{n} V_{j2}} \leq a < \beta.$$

   In the remaining case $\sum_{j=1}^{n} V_{j2} < 0$ we have to show that $\beta < -\|v_1\|_1/\sum_{j=1}^{n} V_{j2}$. Its proof is a consequence of the nonnegativity constraint that $\beta \leq d = -\max_{V_{i2}<0} V_{i1}/V_{i2}$ in combination with the already proved inequality (21). □

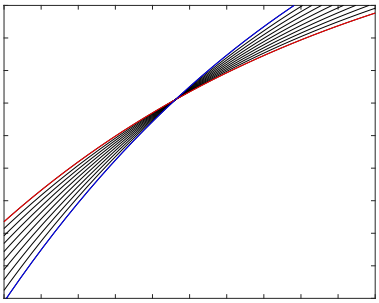

Figure 2: A typical series of feasible profiles with an "isosbestic" point related to the series of feasible spectra. The extremal profiles in blue and red enclose the band of feasible profiles.

Figure 1 illustrates the SCF minimum at (a, c) by a blue dot and the maximum at (b, d) by a red dot. We note that the SCF for the similar analysis using the Frobenius norm takes its minimum and maximum in the same vertices. However, the partial derivative $\partial h/\partial\beta$ in [12], see after Equation (16), is not less than zero but larger than zero. This mistake in [12] affects the position of the maximum and minimum, but has no consequences on the central results as on the band representations since α and β still run through the full intervals $[a, b]$ and $[c, d]$.

2. The bands of feasible profiles are monotone functions of either α or β. This property is a consequence of the solution representation by Eq. (14). The bands of feasible profiles do not depend on the definition of the SCF so that the properties as discussed in detail in Section 3.4 of [12] still hold. The variables α and β run through the full intervals $[a, b]$ respectively $[c, d]$ while connecting the minimum of the SCF at (a, c) and the maximum at (b, d). For a fixed time coordinate (in the case of concentration profiles) or a fixed frequency value (in the case of spectral profiles) the related profile values form either a monotone increasing functions or monotone decreasing functions of α or β or are constant. The latter case resembles an isosbestic point (with respect to the set of feasible profiles instead of relating to the time series of spectra) which occurs for a vanishing derivative. Fig. 2 illustrates a typical series of feasible profiles with such a point.

4. The SCF for the entrywise maximum norm

The entrywise maximum norm (which we write by a triple-lined norm symbol)

$$|||M|||_\infty = \max_{\substack{i=1,\dots,k\\ j=1,\dots,n}} |m_{ij}|$$

is also a matrix norm for $k \times n$ matrices. The norm can easily be evaluated for the rank-1 matrix cs^T since

$$|||cs^T|||_\infty = \max_{\substack{i=1,\dots,k\\ j=1,\dots,n}} |c_i s_j| = \|c\|_\infty \|s\|_\infty. \tag{23}$$

The entrywise maximum norm of cs^T equals the product of the maximum norms of c and s.

The mathematical analysis of the SCF for the entrywise maximum norm seems to be more complex than the analysis of the entrywise 1-norm in Section 3. We get for the dependence of the numerator on α and β

$$\begin{aligned} h_1(\alpha,\beta) = \|c_1\|_\infty \|s_1\|_\infty &= \frac{1}{\beta-\alpha} \|\beta\sigma_1 u_1 - \sigma_2 u_2\|_\infty \|v_1 + \alpha v_2\|_\infty \\ &= \max_{i=1,\dots,k} (\beta\sigma_1 U_{i1} - \sigma_2 U_{i2}) \max_{j=1,\dots,n} \left(V_{j1} + \alpha V_{j2}\right). \end{aligned}$$

Therein the absolute values can be skipped on the given restrictions on α and β which guarantee the componentwise nonnegativity of the vectors whose maximum norms are considered. Unfortunately, the indices in which the maxima are attained depend on α and β. This complicates the mathematical analysis by partial derivatives with respect to α and β. However, our numerical experiments indicate that the entrywise maximum norm for the SCF in the case of systems with two chemical components may have a similar behavior to that studied in Section 3.

5. Numerical studies

This section illustrates properties of the SCF for model data and experimental data.

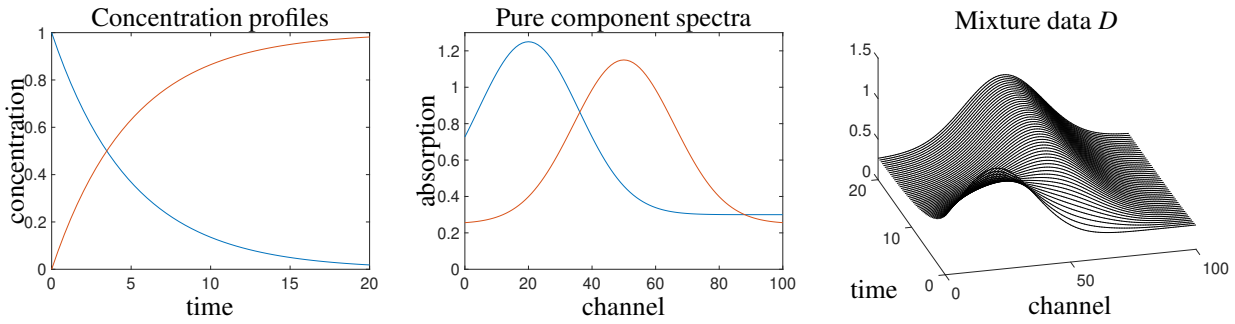

Figure 3: The profiles of the model data set: spectra (left), concentration profiles (middle) and mixture data (right).

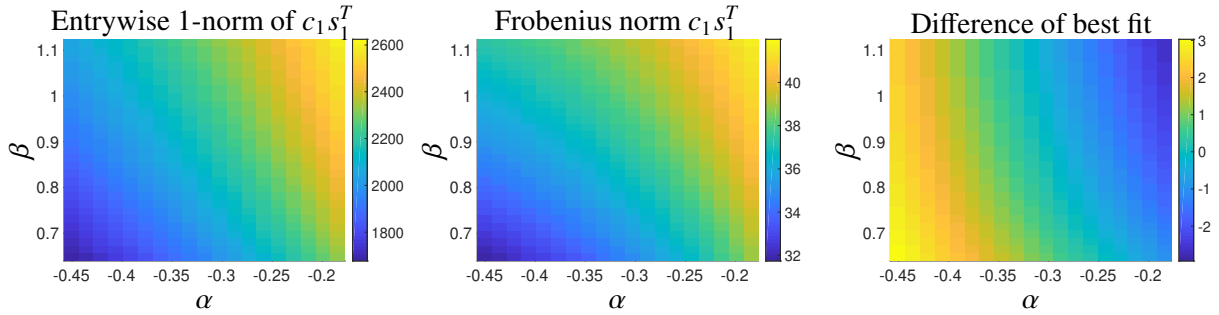

Figure 4: The SCF for the two-component model problem shows a qualitatively similar behavior of the 1-norm (left) compared to the Frobenius norm (center). The best-fit difference plot (right) illustrates differences, but these differences do nit change the position of the minima and maxima.

5.1. Model data

Next a two-component model problem serves to illustrate the typical shape of the SCF for the entrywise 1-norm and the Frobenius norm. The concentration factor of this model problem derives from a discretization of the kinetic model $A \xrightarrow{0.2} B$ on the time interval $[0, 20]$ with $k = 51$ grid points. The pure component spectra are Gaussians

$$s_1(\lambda) = 0.95 \exp(-\frac{(\lambda - 20)^2}{500}) + 0.3, \qquad s_2(\lambda) = 0.9 \exp(-\frac{(\lambda - 50)^2}{500}) + 0.25.$$

Equidistant sampling on $[0, 100]$ with $n = 101$ nodes gives the spectral factor. The product of these factors yields the 51×101 spectral data matrix that is also a part of the FACPACK software [21] as file *example1.mat*. The profiles and the mixed data set are plotted in Fig. 3.

Fig. 4 in the left plot shows the entrywise 1-norm of $c_1 s_1^T$ according to (14) and also the Frobenius norm (see middle plot). The function values for the entrywise 1-norm vary within the interval $[1.68 \cdot 10^3, 2.62 \cdot 10^3]$ and for the Frobenius norm in $[31.74, 41.99]$. Apart from a different scaling of these functions, the color coding suggests a similar qualitative behavior. In order to highlight differences a best fit difference plot is computed as follows: If the numerical values representing these functions are stored in matrices X and Y, then the smallest sum-of-squares of the best fit $\omega X - Y$ is taken in $\omega = X. * Y / \|X\|_F^2$, where $X. * Y$ denotes the entrywise Euclidean inner product of the matrices X and Y. Fig. 4 shows in the right plot the best fit difference plot. Differences can be stated, but they do not change the position of the minima and maxima. For both norms the minimum is attained in lower left vertex and the maximum in the upper right vertex.

Additionally, Fig. 5 illustrates for the same model problem the relative signal contribution $\|c\|_i / \|C\|_i$ according to Eq. (10) subject to the scaling condition that the Euclidean norms of all associated spectra equal 1. The left plot displays the case $i = 1$ (pair of 1-vector norm and 1-matrix norm) and the right plot shows the case $i = 2$ (the Euclidean vector norm and the 2-matrix norm). The plots indicate that the minimum and maximum are again taken in the same vertices of the (α, β) rectangle of feasible parameters as the SCF does for the entrywise 1-norm and the Frobenius norm. Here we do not present a deepened analysis of the relative signal contribution measure by Eq. (10).

5.2. Experimental data

A two-component experimental example is examined in this section, involving a set of calibration samples containing a single analyte, and additional test samples containing the analyte and a single interfering component. The

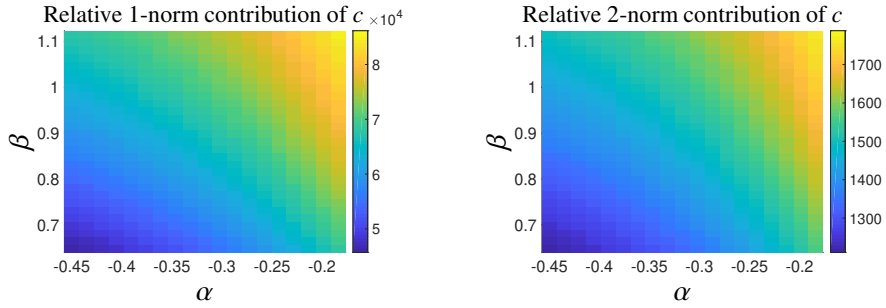

Figure 5: Plots of the relative signal contribution $\|c\|_i/\|C\|_i$ for the two-component model problem. The left plot for $i = 1$, the 1-norm, and the right plot for $i = 2$, the 2-norm, show qualitatively similar results compared to the behavior of the SCF for the entrywise 1-norm and for the Frobenius norm.

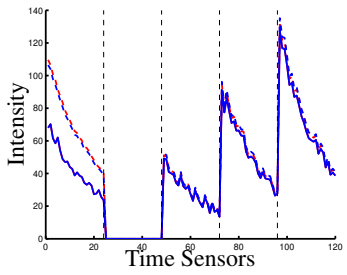

Figure 6: Extreme augmented time decay profiles for the analyte, estimated using N-BANDS for the processing of a typical test sample in the experimental data set. Solid lines correspond to profiles of minimal norm, dashed lines for maximal norm. Blue profiles are for extreme values of $\|cs^T\|_F/\|CS^T\|_F$, red profiles for $\|\|cs^T\|\|_1$. The vertical dashed black lines separate the sub-profiles for each sample: the first one on the left is the test sample and the subsequent ones the calibration samples.

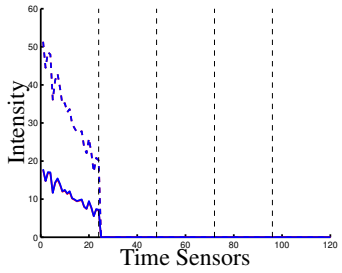

Figure 7: Extreme augmented time decay profiles for the interferent, estimated using N-BANDS. Solid lines correspond to profiles of minimal norm, dashed lines for maximal norm. Blue profiles are for extreme values of $\|cs^T\|_F/\|CS^T\|_F$, red profiles for $\|\|cs^T\|\|_1$. The vertical dashed black lines separate the sub-profiles for each sample: the first one on the left is the test sample and the subsequent ones are the calibration samples, where the interferent is absent. These profiles are almost identical after scaling them to unit 2-norm.

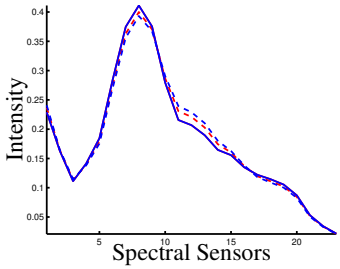

Figure 8: Extreme spectral profiles for the analyte, estimated using N-BANDS. Solid lines correspond to profiles of minimal norm, dashed lines for maximal norm. Blue profiles are for extreme values of $\|cs^T\|_F/\|CS^T\|_F$, red profiles for $\|\|cs^T\|\|_1$.

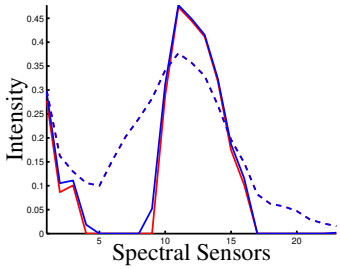

Figure 9: Extreme spectral profiles for the interferent, estimated using N-BANDS. Solid lines correspond to profiles of minimal norm, dashed lines for maximal norm. Blue profiles are for extreme values of $\|cs^T\|_F/\|CS^T\|_F$, red profiles for $\|\|cs^T\|\|_1$.

original data collection and its processing for analyte quantification have already been published, although no rotational ambiguity analysis was carried out at the time [11]. Subsequently, the system was shown to display a substantial degree of ambiguity, due to the fact that analyte and interferent profiles are identical in the concentration mode [3].

Briefly, these data involve the measurement of luminescence excitation-time decay matrices sensitized by terbium(III). Ten test samples were produced from human sera spiked with the fluoroquinolone antibiotic ciprofloxacin and also with a potential interferent (salicylate). The analyte concentrations were within the therapeutic range, i.e., 0-6 mg L^{-1} in serum, with concentrations in the measuring cell of 0, 0.08, 0.16 and 0.24 mg L^{-1}. Individual matrix sizes were 24 data points in the time decay mode and 23 in the spectral mode. For additional experimental details, see [11].

Extreme profiles corresponding to maximum and minimum values of different norms were estimated, namely: (1) the relative Frobenius norm $\|cs^T\|_F/\|CS^T\|_F$, (2) the entrywise 1-norm $\|\|cs^T\|\|_1$ and (3) the relative signal function $\|c\|/\|C\|$ subject to $\|s\|_2 = 1$. Since the present experimental data are rather noisy, negative entries occur in the data matrices, and thus it is important to consider how the available algorithms for computing the band boundaries handle these negative values. The recently published N-BANDS method was adopted here, because it provides non-negative component profiles and consistent results for increasing levels of noise [13]. N-BANDS can be adapted to minimize or maximize any of the three parameters mentioned above.

The analysis of a typical test sample included the following activities: (1) joining the test sample data matrix with those for the calibration samples along the time decay direction (this is the mode representing component concentrations), building an augmented data matrix of size 12023 data points, (2) decomposing the augmented matrix using multivariate curve resolution - alternating least-squares (MCR-ALS) [24] under the constraints of non-negativity and sample selectivity (also called species correspondence), and (3) using the retrieved spectral and time decay profiles as starting values for N-BANDS estimation of band boundaries [13].

For one of the analyzed test samples, the results for the analyte and the interferent are respectively shown in Fig. 6 and Fig. 7 in the time decay mode, and in Fig. 8 and Fig. 9 in the spectral mode (spectra are scaled to unit 2-norm). Profiles for extreme values of the relative signal function $\|c\|/\|C\|$ (not shown) are identical to those for the entrywise 1-norm $\|\|cs^T\|\|_1$. As can be seen, a significant degree of rotational ambiguity exists for the analyte in the time decay mode (Fig. 6) and for the interferent in the spectral mode (Fig. 9). The analyte spectrum is almost unique (Fig. 8), as the interferent time profile, for which the ambiguity is only due to the scale (Fig. 7). In the ideal, noiseless case, the latter profiles will be uniquely defined. This complementary result is tied to the duality principle [15]. It is apparent in these figures that the band boundaries estimated for extreme values of $\|cs^T\|_F/\|CS^T\|_F$ or $\|\|cs^T\|\|_1$ are very similar, with small differences which are most probably due to the presence of instrumental noise.

To discuss the chemical interpretability of the results in an analytical chemistry context, values of the signal contribution functions have been estimated for the ten samples of the test set. The specific values for the relative Frobenis norm $\|csT\|_F/\|\|CS^T\|_F$ corresponding to the extreme band boundaries are given in Table 1. In general, the differences between maximum and minimum values appear to indicate a small degree of ambiguity. However, this is because the analyte spectral profile is almost uniquely recovered, and the augmented concentration profile is mainly dominated by the calibration samples, where the analyte profiles are also nearly unique. Overall, therefore, the extreme values of the signal contribution function in this case do not reflect the degree of rotational ambiguity which is clearly present in the test sample in Fig. 6, which is a representative example for the remaining samples.

On the other hand, the values of $\|\|cs^T\|\|_1$ in Table 2 are appealing from the chemical point of view, since they can be directly related to analyte concentrations. Specifically, the difference between maximum and minimum values can be traced to the uncertainty in the estimated analyte concentration for the test sample. This can be done by isolating, from the total difference between maximum and minimum function values, the portion ascribed to the test sample (Table 2). To convert these differences into absolute concentration errors, the slope of the calibration line of $\|\|cs^T\|\|_1$ vs. nominal analyte concentration is required (see above), and this is shown in Table 2. In relative terms with respect

Sample	Maximum	Minimum	Difference
1	0.997	0.050	0.047
2	0.994	0.939	0.055
3	0.994	0.943	0.051
4	0.969	0.812	0.157
5	0.992	0.990	0.002
6	0.993	0.931	0.062
7	0.978	0.853	0.125
8	0.995	0.975	0.020
9	0.990	0.901	0.089
10	0.989	0.940	0.049

Table 1: Extreme values of the parameter $\|csT\|_F/\|CST\|_F$ when estimating the band boundaries, and the difference between maximum and minimum for each test sample.

Sample	Maximum	Minimum	Difference	Difference for test sample[a]	Absolute error (in mg L^{-1})[b]	Relative error (%)[c]
1	$2.45 \cdot 10^4$	$2.18 \cdot 10^4$	$2.8 \cdot 10^3$	$1.2 \cdot 10^3$	0.036	30
2	$2.22 \cdot 10^4$	$1.96 \cdot 10^4$	$2.6 \cdot 10^3$	$1.3 \cdot 10^3$	0.040	33
3	$2.51 \cdot 10^4$	$2.22 \cdot 10^4$	$2.8 \cdot 10^3$	$1.2 \cdot 10^3$	0.038	32
4	$2.32 \cdot 10^4$	$1.72 \cdot 10^4$	$6.0 \cdot 10^3$	$4.7 \cdot 10^3$	0.14	118
5	$1.75 \cdot 10^4$	$1.53 \cdot 10^4$	$2.1 \cdot 10^3$	$1.3 \cdot 10^3$	0.040	33
6	$2.38 \cdot 10^4$	$2.11 \cdot 10^4$	$2.7 \cdot 10^3$	$1.4 \cdot 10^3$	0.041	34
7	$2.21 \cdot 10^4$	$1.68 \cdot 10^4$	$5.3 \cdot 10^3$	$4.0 \cdot 10^3$	0.12	102
8	$2.29 \cdot 10^4$	$2.03 \cdot 10^4$	$2.6 \cdot 10^3$	$1.4 \cdot 10^3$	0.042	35
9	$2.37 \cdot 10^4$	$2.04 \cdot 10^4$	$3.3 \cdot 10^3$	$2.0 \cdot 10^3$	0.060	50
10	$1.99 \cdot 10^4$	$1.65 \cdot 10^4$	$3.4 \cdot 10^3$	$2.5 \cdot 10^3$	0.076	63

Table 2: Extreme values of the parameter $\|\|\|cs^T\|\|\|_1$ when estimating the band boundaries in the experimental data set, differences attributed to the test samples and the corresponding concentration errors in analyte prediction.
[a] Portion of the difference between maximum and minimum $\|\|\|cs^T\|\|\|_1$ corresponding to the test sample.
[b] Absolute errors are given by the ratio of the difference for the test sample to the slope of the calibration line.
[c] Relative errors are given in % with respect to the mean calibration concentration.

to the mean analyte calibration concentration, the errors range from 30% to more than 100%. They imply a significant impact of rotational ambiguity in analyte prediction, as qualitatively gathered from Fig. 6 for a typical test sample.

Using the extreme values of the relative function $\|c\|/\|C\|$, similar concentration errors as those quoted in Table 2 are found, indicating that this approach also provides an improved analytical interpretation of the consequences of rotational ambiguity.

6. Conclusion

We conclude that Gemperline's primal work on approximating the ranges of feasible bands by means of finding the minimum and maximum of the SCF (1) is still meaningful as far as the (simple) sums are substituted by sums of absolute values. This amounts to using the entrywise 1-norm in the definition of the respective SCF. For experimental spectral data with partially negative entries (e.g. due to baseline or background subtractions) the entrywise 1-norm approach provides results comparable to Tauler's square-summed SCF. The interesting property, namely that for chemical systems with only two-species the respective SCFs take their extrema on the boundary of the sets of feasible coefficients, holds in mathematically precise form for each of the two approaches. This includes the important property that the associated profiles of these extrema exactly enclose the ranges of all feasible nonnegative profiles. The analysis of this paper also indicates that the Frobenius norm and also the entrywise 1-norm are particularly suitable for the evaluation of the signal contribution of the ℓ-th chemical species by means of considering norms of the rank-1 matrices $c_\ell s_\ell^T$. Potentially, the considerations made here can revive Gemperline's approach in combination with absolute values and may additionally allow a more direct interpretation of the widths of feasible bands in terms of uncertainties in concentration values or absorptivities. Finally, we expect that the strict mathematical analysis as presented here for chemical systems with two species cannot be generalized in a straightforward way to systems with more than two components. The reason is, that not only the SCF-function gains in complexity with growing

dimension, but - much more decisive - that the set over which the optimization is executed becomes considerably more complicated. For two components the feasible solutions can be represented with respect to the rectangle (16) for which the boundary points are analytically determined by (17). In contrast to this, the set of feasible solutions for systems with three or more chemical components depends on the area of feasible solutions (AFS), for which no closed-form analytical representation is available. Moreover, the investigations in Section 4 of [12] indicate that a comparable result, namely that the SCF for three-component systems takes its extrema on the boundary of the set of feasible solutions, cannot be expected in general situations.

A. An inequality on vector components

Theorem A.1. *Let $x, y \in \mathbb{R}^m$ and $y > 0$ (componentwise positive). Then it holds that*

$$\min_{i=1,\dots,m} \frac{x_i}{y_i} \leq \frac{\sum_{i=1}^m x_i}{\sum_{i=1}^m y_i} \leq \max_{i=1,\dots,m} \frac{x_i}{y_i}. \tag{24}$$

Proof: We first prove the left inequality. To this end, we show that for any real numbers α, β, γ and δ with $\gamma, \delta > 0$ it holds that

$$\min\left(\frac{\alpha}{\gamma}, \frac{\beta}{\delta}\right) \leq \frac{\alpha+\beta}{\gamma+\delta}. \tag{25}$$

If the latter inequality were wrong, then it would hold

$$\frac{\alpha}{\gamma} > \frac{\alpha+\beta}{\gamma+\delta} \quad \text{and} \quad \frac{\beta}{\delta} > \frac{\alpha+\beta}{\gamma+\delta}.$$

Since $\gamma, \delta > 0$ the two last inequalities are equivalent to

$$\alpha(\gamma+\delta) > (\alpha+\beta)\gamma \quad \text{and} \quad \beta(\gamma+\delta) > (\alpha+\beta)\delta.$$

Simplification yields

$$\alpha\delta > \beta\gamma \quad \text{and} \quad \beta\gamma > \alpha\delta$$

so that $\alpha\delta > \alpha\delta$ which is not true. Hence (25) must be true. By repeated application of (25) we get

$$\begin{aligned} \frac{\sum_{i=1}^m x_i}{\sum_{i=1}^m y_i} &= \frac{x_1 + \sum_{i=2}^m x_i}{y_1 + \sum_{i=2}^m y_i} \geq \min\left(\frac{x_1}{y_1}, \frac{\sum_{i=2}^m x_i}{\sum_{i=2}^m y_i}\right) \geq \min\left(\frac{x_1}{y_1}, \min\left(\frac{x_2}{y_2}, \frac{\sum_{i=3}^m x_i}{\sum_{i=3}^m y_i}\right)\right) \\ &= \min\left(\frac{x_1}{y_1}, \frac{x_2}{y_2}, \frac{\sum_{i=3}^m x_i}{\sum_{i=3}^m y_i}\right) \geq \cdots \geq \min_{i=1,\dots,m} \frac{x_i}{y_i} \end{aligned} \tag{26}$$

which proves the left inequality of the proposition. The right inequality in (24) is proved similarly starting with the pendant of (25)

$$\frac{\alpha+\beta}{\gamma+\delta} \leq \max\left(\frac{\alpha}{\gamma}, \frac{\beta}{\delta}\right)$$

and its subsequent repeated application as in Equation (26). □

Theorem A.2. *Let $x, y \in \mathbb{R}^m$ and $x > 0$ (componentwise positive). Further let $\sum_{i=1}^k y_i \neq 0$.*

1. *If $\sum_{i=1}^m y_i > 0$, then it holds that*

$$\min_{i \text{ with } y_i > 0} \frac{x_i}{y_i} \leq \frac{\|x\|_1}{\sum_{i=1}^m y_i}. \tag{27}$$

2. *If otherwise $\sum_{i=1}^m y_i < 0$, then it holds that*

$$\frac{\|x\|_1}{\sum_{i=1}^m y_i} \leq \max_{i \text{ with } y_i < 0} \frac{x_i}{y_i}. \tag{28}$$

Proof: Let $\mathcal{I}$ be the set of all indexes for which $y_i > 0$. Then Theorem A.1 proves the left inequality of

$$\min_{i \in \mathcal{I}} \frac{x_i}{y_i} \leq \frac{\sum_{i \in \mathcal{I}} x_i}{\sum_{i \in \mathcal{I}} y_i} \leq \frac{\|x_i\|_1}{\sum_{i \in \mathcal{I}} y_i}. \tag{29}$$

Since $0 < \sum_{i=1}^{m} y_i \leq \sum_{i \in \mathcal{I}} y_i$ we get from (29) the inequality (27) by decreasing the denominator of the right-hand side.

In order to prove (28) we multiply (27) by -1 and get reversely written

$$\frac{\|x\|_1}{\sum_{i=1}^{m} -y_i} \leq - \min_{i \text{ with } y_i>0} \frac{x_i}{y_i} = \max_{i \text{ with } y_i>0} \frac{x_i}{-y_i}.$$

By substituting $-y \to z$ we get

$$\frac{\|x\|_1}{\sum_{i=1}^{m} z_i} \leq \max_{i \text{ with } z_i<0} \frac{x_i}{z_i}$$

which proves (28). □

References

[1] H. Abdollahi, M. Maeder, and R. Tauler. Calculation and meaning of feasible band boundaries in multivariate curve resolution of a two-component system. *Anal. Chem.*, 81(6):2115–2122, 2009.

[2] H. Abdollahi and R. Tauler. Uniqueness and rotation ambiguities in multivariate curve resolution methods. *Chemom. Intell. Lab. Syst.*, 108(2):100–111, 2011.

[3] G. Ahmadi and H. Abdollahi. A systematic study on the accuracy of chemical quantitative analysis using soft modeling methods. *Chemom. Intell. Lab. Syst.*, 120:59 – 70, 2013.

[4] O.S. Borgen and B.R. Kowalski. An extension of the multivariate component-resolution method to three components. *Anal. Chim. Acta*, 174:1–26, 1985.

[5] P.J. Gemperline. Computation of the range of feasible solutions in self-modeling curve resolution algorithms. *Anal. Chem.*, 71(23):5398–5404, 1999.

[6] A. Golshan, H. Abdollahi, and M. Maeder. Resolution of rotational ambiguity for three-component systems. *Anal. Chem.*, 83(3):836–841, 2011.

[7] A. Golshan, M. Maeder, and H. Abdollahi. Determination and visualization of rotational ambiguity in four-component systems. *Anal. Chim. Acta*, 796(0):20–26, 2013.

[8] G.H. Golub and C.F. Van Loan. *Matrix Computations*. Johns Hopkins Studies in the Mathematical Sciences. Johns Hopkins University Press, Baltimore, MD, 2012.

[9] J. Jaumot and R. Tauler. MCR-BANDS: A user friendly MATLAB program for the evaluation of rotation ambiguities in multivariate curve resolution. *Chemom. Intell. Lab. Syst.*, 103(2):96–107, 2010.

[10] A. Jürß, M. Sawall, and K. Neymeyr. On generalized Borgen plots. I: From convex to affine combinations and applications to spectral data. *J. Chemom.*, 29(7):420–433, 2015.

[11] V.A. Lozano, G.A. Ibañez, and A.C. Olivieri. Second-order analyte quantitation under identical profiles in one data dimension. A dependency-adapted partial least-squares/residual bilinearization method. *Anal. Chem.*, 82(11):4510–4519, 2010.

[12] K. Neymeyr, A. Golshan, K. Engel, R. Tauler, and M. Sawall. Does the signal contribution function attain its extrema in boundary points of the area of feasible solutions? *Chemom. Intell. Lab. Syst.*, 196:103887e, 2020.

[13] A.C. Olivieri and R. Tauler. N-BANDS: A new algorithm for estimating the extension of feasible bands in multivariate curve resolution of multi-component systems in the presence of noise and rotational ambiguity, 2020. (in press, DOI 10.1002/cem.3317).

[14] N. Omidikia, M. Ghaffari, and R. Rajkó. Sparse non-negative multivariate curve resolution: L0, L1, or L2 norms? *Chemom. Intell. Lab. Syst.*, 199:103969, 2020.

[15] R. Rajkó. Natural duality in minimal constrained self modeling curve resolution. *J. Chemom.*, 20(3-4):164–169, 2006.

[16] R. Rajkó. Studies on the adaptability of different Borgen norms applied in self-modeling curve resolution (SMCR) method. *J. Chemom.*, 23(6):265–274, 2009.

[17] R. Rajkó. Additional knowledge for determining and interpreting feasible band boundaries in self-modeling/multivariate curve resolution of two-component systems. *Anal. Chim. Acta*, 661(2):129–132, 2010.

[18] R. Rajkó and K. István. Analytical solution for determining feasible regions of self-modeling curve resolution (SMCR) method based on computational geometry. *J. Chemom.*, 19(8):448–463, 2005.

[19] M. Sawall, A. Jürß, H. Schröder, and K. Neymeyr. Simultaneous construction of dual Borgen plots. I: The case of noise-free data. *J. Chemom.*, 31:e2954, 2017.

[20] M. Sawall, C. Kubis, D. Selent, A. Börner, and K. Neymeyr. A fast polygon inflation algorithm to compute the area of feasible solutions for three-component systems. I: Concepts and applications. *J. Chemom.*, 27:106–116, 2013.

[21] M. Sawall, A. Moog, and K. Neymeyr. FACPACK: A software for the computation of multi-component factorizations and the area of feasible solutions, Revision 1.3. FACPACK homepage: http://www.math.uni-rostock.de/facpack/, 2018.

[22] M. Sawall and K. Neymeyr. A fast polygon inflation algorithm to compute the area of feasible solutions for three-component systems. II: Theoretical foundation, inverse polygon inflation, and FAC-PACK implementation. *J. Chemom.*, 28:633–644, 2014.

[23] M. Sawall and K. Neymeyr. A ray casting method for the computation of the area of feasible solutions for multicomponent systems: Theory, applications and FACPACK-implementation. *Anal. Chim. Acta*, 960:40–52, 2017.

[24] R. Tauler. Multivariate curve resolution applied to second order data. *Chemom. Intell. Lab. Syst.*, 30(1):133 – 146, 1995.

[25] R. Tauler. Calculation of maximum and minimum band boundaries of feasible solutions for species profiles obtained by multivariate curve resolution. *J. Chemom.*, 15(8):627–646, 2001.

[26] R.S. Varga. *Matrix Iterative Analysis*. Springer Series in Computational Mathematics. Springer Berlin Heidelberg, 1999.